Theor Appl Climatol (2014) 117:643–652
DOI 10.1007/s00704-013-1035-5

ORIGINAL PAPER

Using MODIS and AVHRR data to determine regional surface heating field and heat flux distributions over the heterogeneous landscape of the Tibetan Plateau

Yaoming Ma · Cunbo Han · Lei Zhong · Binbin Wang · Zhikun Zhu · Yongjie Wang · Lang Zhang · Chunchun Meng · Chao Xu · Pukar Man Amatya

Received: 3 December 2012 / Accepted: 13 October 2013 / Published online: 26 October 2013

Abstract In this study, a parameterization methodology based on Advanced Very High-Resolution Radiometer (AVHRR), Moderate Resolution Imaging Spectroradiometer (MODIS), and in situ data is proposed and tested for deriving the regional surface heating field, sensible heat flux, and latent heat flux over a heterogeneous landscape. In this case study, this method is applied to the whole Tibetan Plateau (TP) area. Four sets of AVHRR data and four sets of MODIS data (collected on 17 January 2003, 14 April 2003, 23 July 2003, and 16 October 2003) were used in this study to make comparisons between winter, spring, summer, and autumn values. The satellite-derived results were also validated using the "ground truth" as measured in the stations of CAMP/Tibet (Coordinated Enhanced Observing Period (CEOP) and Asia–Australia Monsoon Project on the Tibetan Plateau). The results show that the surface heating field, sensible heat flux, and latent heat flux in the four seasons across the TP are in close accordance with its land surface status. These parameters range widely due to the strongly contrasting surface features found within the TP region. Also, the estimated surface heating field, sensible heat flux, and latent heat flux all agree with the ground truth data, and usually, the absolute percentage difference between the two sets of data is less than 10 % at the validation stations. The AVHRR results were also in agreement with the MODIS data, with the latter usually displaying a higher level of accuracy. We have thus concluded that the proposed method was successful in retrieving surface heating field, sensible heat flux, and latent heat flux values using AVHRR, MODIS, and in situ data over the heterogeneous land surface of the TP. Shortcomings and possible further improvements in the method are also discussed.

Y. Ma (✉) · C. Han · L. Zhong · B. Wang · Z. Zhu · Y. Wang · L. Zhang · C. Meng · C. Xu · P. M. Amatya
Key Laboratory of Tibetan Environment Changes and Land Surface Processes, Institute of Tibetan Plateau Research, Chinese Academy of Sciences, Beijing, China
e-mail: ymma@itpcas.ac.cn

Y. Ma · C. Han · B. Wang · Z. Zhu · L. Zhang · C. Meng · C. Xu
Qomolangma Station for Atmospheric and Environmental Observation and Research, Chinese Academy of Sciences, Dingri, Tibet, China

C. Han · B. Wang · Z. Zhu · L. Zhang · C. Meng · C. Xu · P. M. Amatya
University of Chinese Academy of Sciences, Beijing 100049, China

L. Zhong
International Institute for Geo-Information Science and Earth Observation, Enschede, The Netherlands

L. Zhong
School of Earth and Space Sciences, University of Science and Technology of China, Hefei, China

1 Introduction

The Tibetan Plateau (TP) is located in the central eastern Eurasian continental mass and contains the world's highest average elevation (circa 4,000 m), with some surface features reaching into the mid-troposphere. It comprises an extensive landmass extending from subtropical to middle latitudes and spans >25° longitude (Fig. 1). Because of its topographic character, the plateau surface absorbs large quantities of solar radiation energy and undergoes dramatic seasonal changes in its surface heat and water fluxes (e.g., Ye and Gao 1979; Ye 1981; Yanai et al. 1992; Ye and Wu 1998; Ma and Tsukamoto 2002; Hsu and Liu 2003; Yang et al. 2004; Ma et al. 2005;

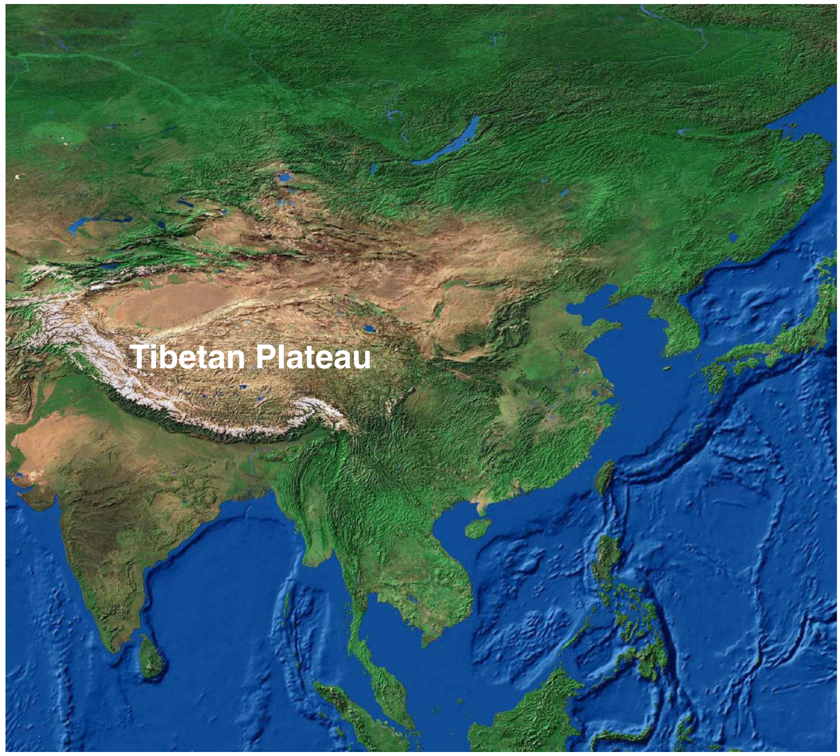

Fig. 1 The location and landscape of the Tibetan Plateau

Sato and Kimura 2007; Ma et al. 2008; Xu et al. 2008; Cui and Graf 2009; Zhong et al. 2010). Many studies have found that the east Asian monsoonal climate and the middle Asian dry climate in summer are intensified by TP mechanical and thermal forcing (e.g., Liu et al. 2007). This heat source enhances the Asian monsoon and further influences precipitation in China and east Asia (e.g., Yanai et al. 1992; Wu and Zhang 1998; Zhao and Chen 2001; Duan et al. 2005; Duan et al. 2011).

The surface heating field has been defined as (Ji et al. 1986):

$$H_{\mathrm{f}} = R_{\mathrm{n}} - G_0 = H + \lambda E \tag{1}$$

where R_{n} is net radiation flux, G_0 is surface soil heat flux, H is sensible heat flux, and λE is latent heat flux. When $H_{\mathrm{f}}>0$, the land surface is a heat source for the atmosphere; otherwise, the land surface is a heat sink for the atmosphere. Therefore, net radiation flux, soil heat flux, sensible heat flux, and latent heat flux are very important components in the distribution of the surface heating field over the TP.

Some researchers have focused upon determining net radiation flux, soil heat flux, sensible heat flux, and latent heat flux by using in situ data (e.g., Ji et al. 1986; Ma and Tsukamoto 2002; Ma et al. 2005; Ma and Ma 2006). Regional distributions of net radiation flux, soil heat flux, sensible heat flux, and latent heat flux over the TP have already been measured by some researchers (e.g., Ma et al. 2002, 2006), though results remain on a mesoscale. In order to understand the effect of the TP on climate change over China, east Asia, and even globally, the regional distribution of net radiation flux, soil heat flux, sensible heat flux, latent heat flux, and the surface heating field over the whole TP has to be accurately determined.

Remote sensing from satellites, in conjunction with data from sparse field experimental stations, offers the possibility of determining the regional distribution of land surface heat fluxes (net radiation flux, soil heat flux, sensible heat flux, and latent heat flux) and the surface heating field over a heterogeneous land surface. The objective of this study is to explore the feasibility of upscaling the point and mesoscale net radiation flux, soil heat flux, sensible heat flux, latent heat flux, and surface heating field to yield distributions quantifiable on a plateau-wide scale with the aid of NOAA (National Oceanic and Atmospheric Administration) Advanced Very High-Resolution Radiometer (AVHRR) data, Moderate Resolution Imaging Spectroradiometer (MODIS) data, and in situ data.

2 Theory and scheme

The general concept governing the methodology is shown in Fig. 2. The surface reflectance for short-wave radiation r_0 and surface temperature T_{sfc} are retrieved from AVHRR and MODIS data by using land surface observations of surface

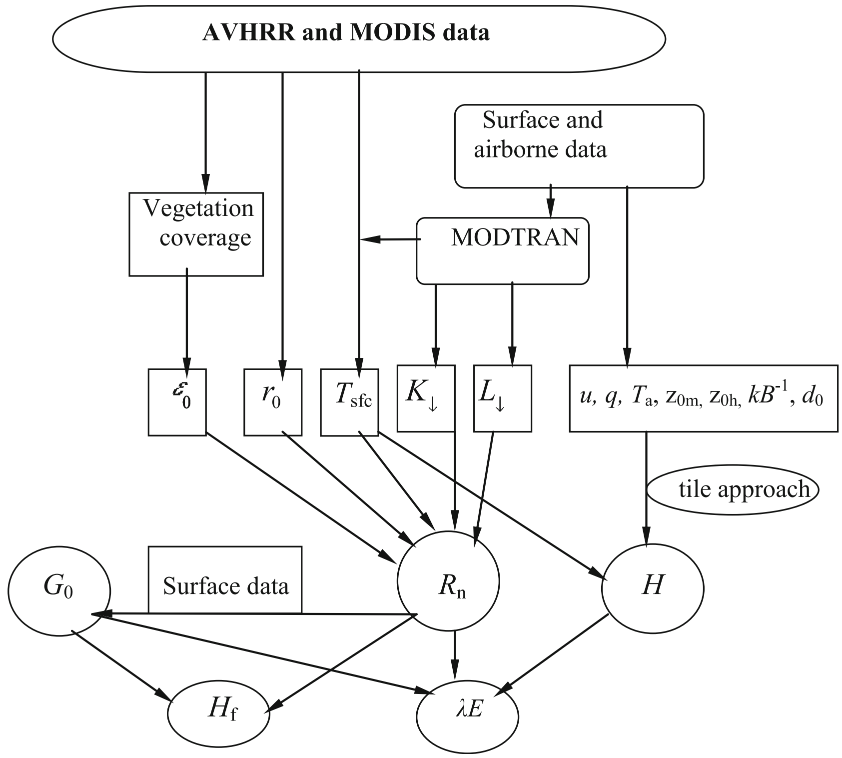

Fig. 2 The diagram of parameterization procedure to determine net radiation flux, soil heat flux, surface heating field, sensible heat flux, and latent heat flux by combining AVHRR and MODIS data with field observations

temperature, surface albedo, and aerological observations of the profiles of water vapor content; wind speed and direction as observed by a radiosonde system; a wind profiler and tethered balloon; the radiative transfer model MODTRAN (Berk et al. 1989); and atmospheric correction. The MODTRAN model computes downward short-wave and long-wave radiations at the surface (Ma and Tsukamoto 2002). After collation of these results, the regional surface net radiation flux $R_n(x,y)$ can be determined. The regional soil heat flux $G_0(x,y)$ is estimated using $R_n(x,y)$ and field observations (Ma et al. 2002). The regional sensible heat flux $H(x,y)$ is estimated using $T_{sfc}(x,y)$ and surface and aerological data captured with the aid of the so-called "tile approach" (Ma et al. 2010). The regional latent heat flux $\lambda E(x,y)$ is calculated as the residual value of the energy budget theorem for land surface heating. The surface heating field $H_f(x,y)$ is derived from $R_n(x,y)$ and $G_0(x,y)$ by using Eq. (1) on a regional scale.

2.1 Net radiation flux

The regional net radiation flux is derived using:

$$R_n(x,y) = (1-r_0(x,y))K_{\downarrow}(x,y) + L_{\downarrow}(x,y) - \varepsilon_0(x,y)\sigma T^4_{sfc}(x,y) \quad (2)$$

where $r_0(x,y)$ is surface reflectance at position (x, y), $\varepsilon_0(x,y)$ is surface emissivity, $T_{sfc}(x,y)$ is surface temperature, $K_{\downarrow}(x,y)$ is incoming short-wave radiation flux density, and $L_{\downarrow}(x,y)$ is incoming long-wave radiation flux. Surface emissivity of $\varepsilon_0(x,y)$ is a function of vegetation coverage. It is derived from the model suggested by Valor and Caselles (1996). The incoming long-wave radiation flux $L_{\downarrow}(x,y)$ and the incoming short-wave radiation flux $K_{\downarrow}(x,y)$ in Eq. (2) are directly calculated from the radiative transfer model MODTRAN by using aerological observations of the profiles of water vapor content, wind speed and direction as observed by a radiosonde system, a wind profiler, and a tethered balloon (Ma and Tsukamoto 2002). The surface reflectance and surface temperature in Eq. (2) are derived in different ways, dependent upon differing sets of remote sensing data. They have been derived using the methodology proposed by Zhong et al. (2010).

2.2 Soil heat flux and surface heating field

The regional soil heat flux $G_0(x,y)$ is determined by (Choudhury and Monteith 1988):

$$G_0(x,y) = \rho_s c_s \left[\left(T_0(x,y) - T_s\left(x,y\right) \right) \right] / r_{sh}(x,y) \quad (3)$$

where ρ_s is soil dry bulk density, c_s is soil specific heat, $T_s\ (x,y)$ stands for soil temperature at a determined depth, and $r_{sh}\ (x,y)$ represents soil heat transfer resistance.

Fig. 3 The distribution maps of surface heating field over the Tibetan Plateau area. **a** AVHRR results and **b** MODIS results

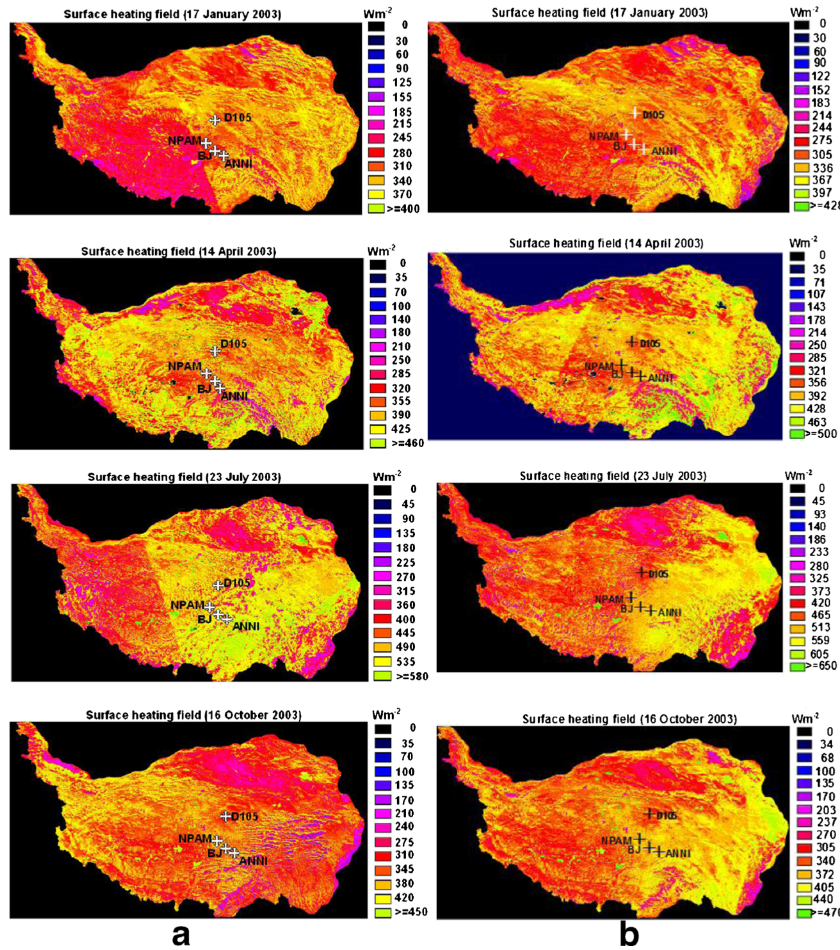

$G_0(x, y)$ cannot be directly mapped from satellite measurements through Eq. (3). The difficulty lies in deriving $r_{sh}(x,y)$ and $T_s(x,y)$ (Bastiaanssen 1995; Wang et al. 1995; Ma and Tsukamoto 2002; Ma et al. 2002, 2006; Gao et al. 2010). In order to calculate the values of $G_0(x, y)$ solely from remote sensing data, these values have to be proportional to another term within the energy balance equation. A good candidate for this proportional term is $R_n(x,y)$ (e.g., Jackson et al. 1985; Choudhury et al. 1987; Kustas and Daughtry 1990; Bastiaanssen 1995; Ma and Tsukamoto 2002; Ma et al. 2006; Gao et al. 2010). Based on the in situ data gathered in the TP, Ma et al. (2002) proposed an equation to derive regional soil heat flux $G_0(x,y)$ from regional net radiation flux $R_n(x,y)$ for the TP, thus:

$$G_0(x,y) = 0.35462(\pm 0.00235)R_n(x,y) - 47.79008(\pm 0.70005) \quad (4)$$

Equation (4) is based on the in situ data gathered from the different land surface types of the TP, and $R_n(x,y)$ in Eq. (4) is similarly dependent upon surface type. Equation (4) has therefore been used in this study to determine the regional distribution of soil heat flux in the TP area.

The regional surface heating field $H_f(x,y)$ may then be derived from Eq. (5) after the determination of $R_n(x,y)$ and $G_0(x,y)$, thus:

$$H_f(x,y) = R_n(x,y) - G_0(x,y) \quad (5)$$

2.3 Sensible heat flux and latent heat flux

The sensible heat flux H is estimated with a bulk transfer equation written in the form (Montheith 1973):

$$H = \rho c_p \frac{T_{sfc} - T_a}{r_{ah}} \quad (6)$$

where r_{ah} is aerodynamic resistance for heat transfer between land surface and reference height, T_{sfc} is the surface temperature, T_a is the air temperature at the reference height, ρ is the air density, and c_p is the air specific heat at constant pressure.

In order to determine the regional distribution of sensible heat flux $H(x,y)$ over the TP, the "tile approach" (Ma et al. 2010) is used here. In the "tile approach," the reference height z_{ref} is taken within the surface layer (SL). Then, using satellite measurements at the surface and the SL observations on a

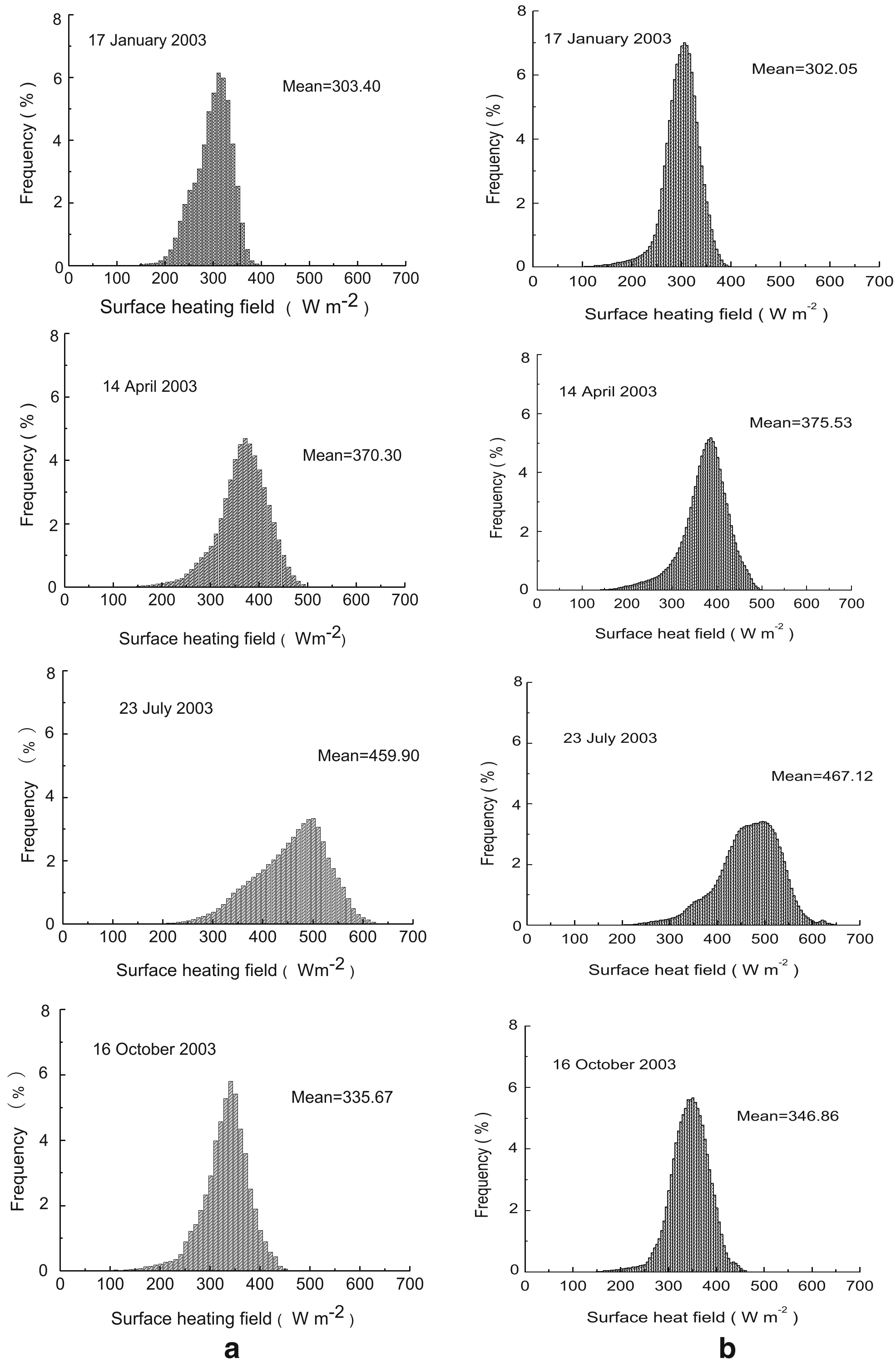

Fig. 4 The frequency distribution of surface heating field over the Tibetan Plateau area. **a** AVHRR results and **b** MODIS results

"tile" at and below the reference height (e.g., 20 m), the heat flux over a heterogeneous landscape is estimated. Firstly, surface reflectance r_0, surface temperature T_{sfc}, vegetation coverage P_{v}, and surface emissivity ε_0 at the surface are derived from satellite measurements. Secondly, SL observations on a "tile" of wind speed u, air temperature T_{a}, and specific humidity q at the reference height are made. Zero-plane displacement d_0, aerodynamic roughness length $z_{0\mathrm{m}}$ and thermodynamic roughness length $z_{0\mathrm{h}}$, excess resistance for heat transportation kB^{-1}, and the like in the SL below the reference height over the i-tile are used to estimate the regional sensible heat flux $H(x,y)$ (Fig. 2).

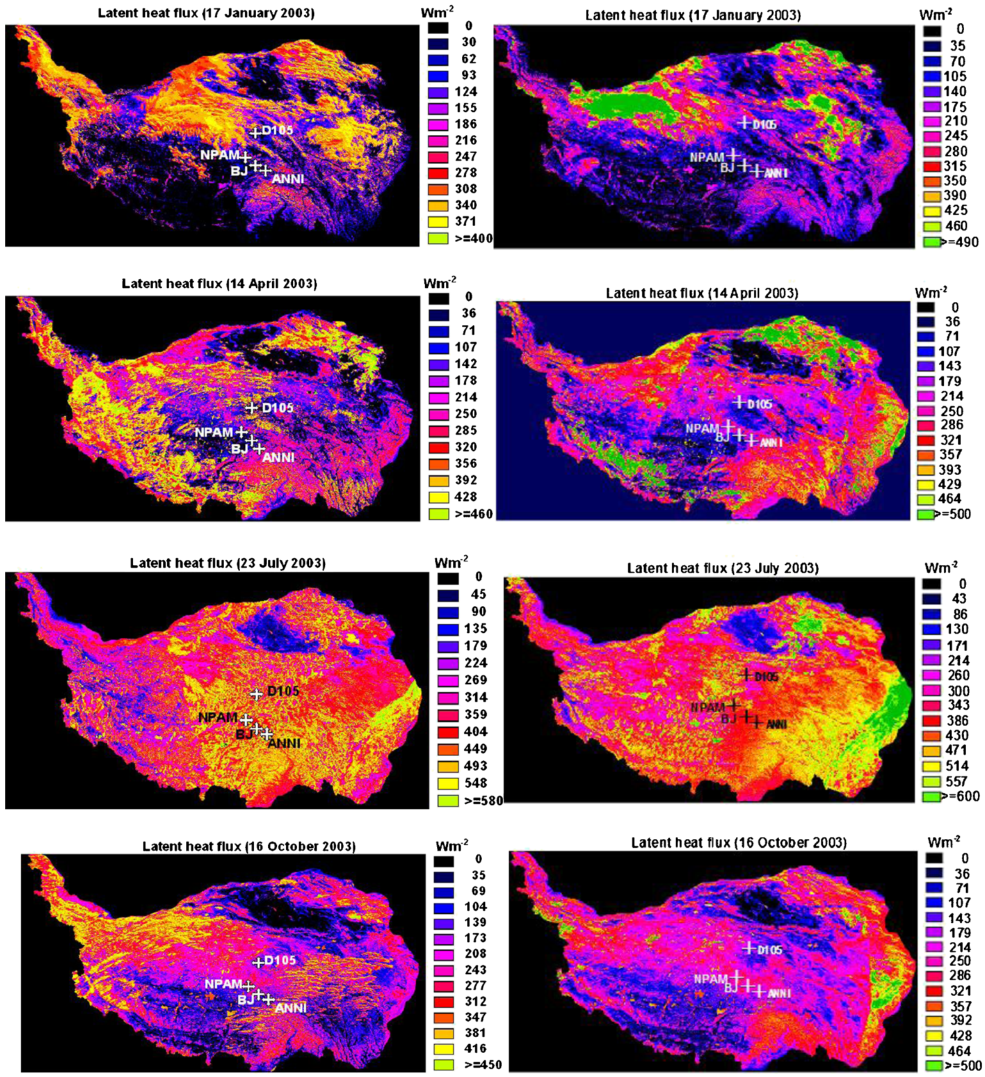

Fig. 5 The distribution maps of latent heat flux over the Tibetan Plateau area. **a** AVHRR results and **b** MODIS results

Hence, in mathematical terms:

$$
\begin{aligned}
H_1(x,y) &= \rho c_p \frac{[T_{sfc}(x,y) - T_{a1}]}{r_{ah1}},\\
H_2(x,y) &= \rho c_p \frac{[T_{sfc}(x,y) - T_{a2}]}{r_{ah2}},\\
&\cdots \qquad \cdots\\
H_n(x,y) &= \rho c_p \frac{[T_{sfc}(x,y) - T_{an}]}{r_{ahn}}
\end{aligned} \tag{7}
$$

Therefore, H over the whole TP may be derived from:

$$H(x,y) = \sum_{i=1}^{n} a(i) H_i(x,y), \tag{8}$$

where $a(i)$ is the fractional ratio of each "tile" for the TP as determined from satellite images and land cover maps. $H_1(x,y)$, $H_2(x,y)$..., and $H_n(x,y)$ are the sensible heat flux calculations on each "tile"; T_{a1}, T_{a2}..., and T_{an} are air temperature measurements at the reference height on each "tile"; and r_{ah1}, r_{ah2} ..., and r_{ahn} are aerodynamic resistance for heat transfer between land surface and the reference height on each "tile". r_{ah1}, r_{ah2} ..., and r_{ahn} are determined from the eddy diffusion coefficients for heat transport between the land surface and the reference height (Ma et al. 2010).

The regional latent heat flux $\lambda E(x,y)$ is derived as the residual value of the energy budget theorem for land surface heating based on the zero horizontal advection conditions, i.e.,

$$\lambda E(x,y) = R_n(x,y) - H(x,y) - G_0(x,y) \tag{9}$$

3 Cases study and validation

Four sets each of AVHRR data and MODIS data for the TP area were used in this study (as the TP covers a large proportion of southwest China, several satellite images are needed to make a composition of the whole plateau image here). They were collected on 17 January 2003 (winter), 14 April 2003 (spring), 23 July 2003 (summer), and 16 October 2003 (autumn).

Inputting the AVHRR, MODIS, and in situ data, the distributions of net radiation flux, soil heat flux, sensible heat flux, latent heat flux, and the surface heating field are derived using Eqs. (2)–(9). Figures 3 and 5 show surface heating field and latent heat flux distribution maps for the TP. Figures 4 and 6 show their distribution frequencies. The surface heating field and latent heat flux distribution maps are based on 3,012×1,517 pixels with a size of 1×1 km. The derived net radiation

Fig. 6 The frequency distribution of latent heat flux over the Tibetan Plateau area. **a** AVHRR results and **b** MODIS results

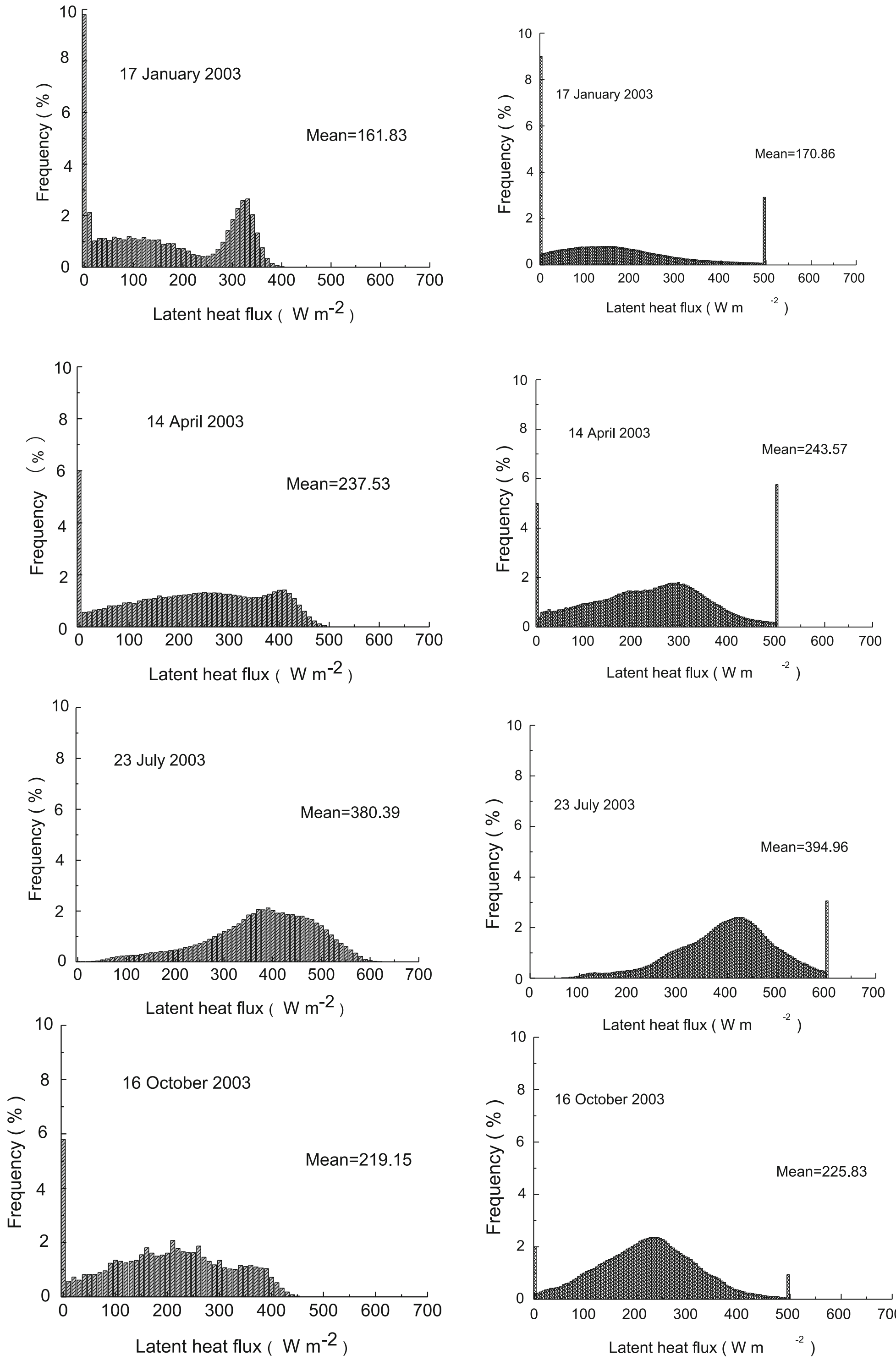

flux, soil heat flux, sensible heat flux, latent heat flux, and surface heating field have been further validated by station measurements. In situ data collected at four CAMP/Tibet stations, viz.: D105 (33.06° N, 91.94° E; elevation of 5, 039 m; sparse meadow land cover); NPAM (31.93° N, 91.71° E; elevation of 4,620 m; grassy marshland land cover); BJ (31.37° N, 91.90° E; elevation of 4,509 m; sparse meadow land cover); and ANNI (31.25° N,92.17° E; elevation of 4,

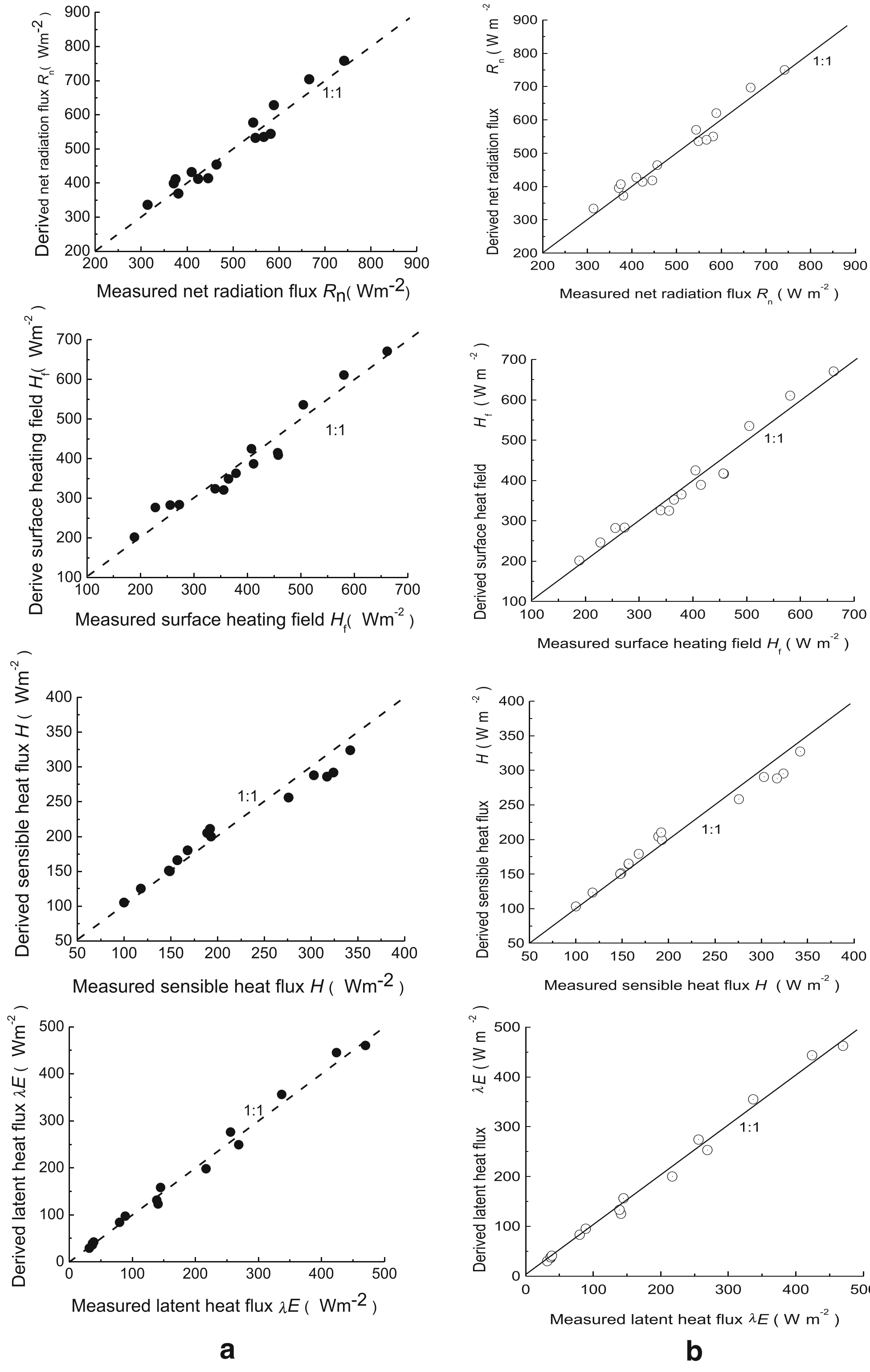

Fig. 7 Comparison of derived results with field measurements for the net radiation flux, surface heating field, sensible heat flux, and latent heat flux over the Tibetan Plateau area, together with a 1:1 line. **a** AVHRR and **b** MODIS

480 m; grassy marshland land cover) were used for the validation in 2003. In Fig. 7, the satellite-derived results are validated against the station measurements. Since it was difficult to determine the locations of the four stations, the values of a 5×5-pixel rectangle surrounding the determined Universal Transfer Macerator (UTM) coordinates are compared with the in situ data. In Fig. 1, the derived results are validated against the measured values collected in the field. The absolute percentage difference (APD) quantitatively measures the difference between the derived results ($H_{\mathrm{derived}(i)}$) from satellite and measured values ($H_{\mathrm{measured}(i)}$) and:

$$APD = \frac{\left|H_{derived(i)} - H_{measured(i)}\right|}{H_{measured(i)}}. \tag{10}$$

where i represents different derived or measured values of R_{n}, G_0, H, and λE at four the validation sites ($i=1\ldots4$).

The results show that: (1) the derived net radiation heat flux (R_{n}), soil heat flux (G_0), sensible heat flux (H), latent heat flux (λE), and surface heating field (H_{f}) derived from MODIS and AVHRR data for the TP are in close accordance with the land surface status; the wide range in values reflects highly contrasting surface features (forests, grasslands, meadows, marshlands, farmland, deserts, desertification zones, snowy mountains, rivers, glaciers, lakes, etc.) in this region (Figs. 1, 3, 4, 5, and 6). One low-value center, located in the desert/desertification zone of the Qaidam Basin, was clearly identifiable in the derived latent heat flux images (Figs. 5 and 6); (2) the derived net radiation flux, soil heat flux, sensible heat flux, latent heat flux, and surface heating field values across the TP are very close to the field measurements. The difference between the derived results and the field observations' APD is less than 10 % (Fig. 7) because accurate surface reflectance and surface temperatures were determined, and the processes within the atmospheric boundary layer were considered in greater detail when determining sensible heat flux values; (3) the mean surface heating field values over the TP increase from January to April and from April to July, decreasing from October to January. They are 303.4 W m^{-2}, 370.3 W m^{-2}, 459.9 W m^{-2}, and 335.67 W m^{-2} for the AVHRR data and 302.1 W m^{-2}, 375.5 W m^{-2}, 467.1 W m^{-2}, and 346.9 W m^{-2} for the MODIS data. The mean latent heat flux values across the TP also increase from January to April and from April to July, decreasing from October to January. They are 161.8 W m^{-2}, 237.5 W m^{-2}, 380.4 W m^{-2}, and 219.1 W m^{-2} for the AVHRR data and 170.9 W m^{-2}, 243.6 W m^{-2}, 395.0 W m^{-2}, and 225.8 W m^{-2} for the MODIS data; and (4) as a rule, the derived results from AVHRR images were in agreement with those from MODIS images when the imaging time was the same. The results collected from the MODIS procedure were usually superior to the AVHRR data, which had an average APD of 5.4 % (net radiation flux), 8.0 % (soil heat flux), 6.3 % (surface heating field), 6.5 % (sensible heat flux), and 6.9 % (latent heat flux), while the values for the MODIS data were 4.9 % (net radiation flux), 7.3 % (soil heat flux), 5.5 % (surface heating field), 5.0 % (sensible heat flux), and 5.7 % (latent heat flux) (Fig. 7).

4 Concluding remarks

In this study, the regional distributions of net radiation heat flux, soil heat flux, sensible heat flux, latent heat flux, and the surface heating field over the heterogeneous landscape of the TP are derived with the aid of AVHRR, MODIS, and in situ data. Compared with reliance upon field measurements alone, the proposed methodology has proven to provide a better approach for deriving related land surface heat flux (net radiation heat flux, soil heat flux, sensible heat flux, and latent heat flux) and the surface heating field over a heterogeneous landscape. It forms a sound basis for the further study of water–heat exchange processes on heterogeneous land surfaces.

Deriving regional net radiation heat flux, soil heat flux, sensible heat flux, latent heat flux, and the surface heating field over a heterogeneous landscape is not straightforward. The parameterization methodology presented in this research is still developing, as only a single set of values from a specific time on a specific day is used in this research. In order to establish more accurate regional values of net radiation heat flux, soil heat flux, sensible heat flux, latent heat flux, and surface heating field values and to delineate their seasonal and annual variations over the TP, there is a need for more field observations, more accurate radiation transfer models for determining surface reflectance and temperatures, and more satellite data such as that provided by the Landsat-5 TM, GMS (Geostationary Meteorological Satellite), ATSR (Along Track Scanning Radiometer), and MODIS systems.

Acknowledgment This work was under the auspices of the Chinese National Key Programme for Developing Basic Sciences (2010CB951701), the Chinese Academy of Sciences (XDB03030201), National Natural Foundation of China (41275010 and 40905017), the External Cooperation Program of the Chinese Academy of Sciences, grant no. GJHZ1207 and EU-FP7 projects "CORE-CLIMAX" (313085), and "CEOP-AEGIS" (212921).

References

Bastiaanssen WGM (1995) Regionalization of surface fluxes and moisture indicators in composite terrain, PhD Thesis. Wageningen Agricultural University, Wageningen, the Netherlands, 273pp

Berk A, Bernstein LS, Robertson DC (1989) MODTRAN: a moderate resolution model for LOTRAN 7, GL-TR-89-0122. Geophysics Laboratory, Hanscom Air Force Base, Bedford, MA

Choudhury BJ, Idso SB, Reginato RJ (1987) Analysis of an empirical model for soil heat flux under a growing wheat crop for estimating evaporation by infrared-temperature based energy balance Eq. Agr Forest Meteorol 39:283–297

Choudhury BJ, Monteith JL (1988) A four-layer model for the heat budget of homogeneous land surfaces. Q J R Meteorol Soc 114:373–398

Cui X-F, Graf H (2009) Recent land cover changes on the Tibetan Plateau: a review. Clim Chang 94:47–61

Duan A-M, Liu Y-M, Wu G-X (2005) Heating status of the Tibetan Plateau from April to June and rainfall and atmospheric circulation anomaly over east Asia in midsummer. Science in China (D) 48:250–257

Duan A-M, Li F-R, Wang M, Wu G-X (2011) Persistent weakening trend in the spring sensible heat source over the Tibetan Plateau and its impact on the Asian summer monsoon. J Clim 24:5671–5682

Gao Z-Q, Horton R, Liu H-P (2010) Impact of wave phase difference between soil surface heat flux and soil surface temperature on soil surface energy balance closure. J Geophys Res 115:D16112. doi:10.1029/2009JD013278

Hsu H, Liu X (2003) Relationship between the Tibetan Plateau heating and east Asian summer monsoon rainfall. Geophysics Research Letters 30:D2066. doi:10.1029/2003GL017909

Jackson RD Jr, Pinter PJ, Reginato RJ (1985) Net radiation calculated from remote multispectral and ground station meteorological data. Agricultural Forest Meteorology 35:153–164

Ji G-L, Yao L-C, Yuan F-M (1986) Characteristics of surface and atmospheric heating fields over Qinghai–Xizang Plateau during the winter in 1982. Science China (B) 29(8):876–888

Kustas WP, Daughtry CST (1990) Estimation of the soil heat flux/net radiation ratio from spectral data. Agric For Meteorol 39:205–223

Liu Y-M, Bao Q, Duan A-M, Qian Z-A, Wu G-X (2007) Recent progress in the impact of the Tibetan Plateau on climate in China. Advanced in Atmospheric Sciences 24(6):1060–1076

Ma W-Q, Ma Y-M (2006) The annual variations on land surface energy in the northern Tibetan Plateau. Environ Geol 50(5):645–650. doi:10.1007/s00254-006-0238-9

Ma Y-M, Tsukamoto O (2002) Combining satellite remote sensing with field observations for land surface heat fluxes over inhomogeneous landscape. China Meteorological Press, Beijing

Ma Y-M, Su Z-B, Li Z-L, Koike T, Menenti M (2002) Determination of regional net radiation and soil heat flux densities over heterogeneous landscape of the Tibetan Plateau. Hydrol Process 16(15):2963–2971

Ma Y-M, Fan S-H, Ishikawa H, Tsukamoto O, Yao T-D (2005) Diurnal and inter-monthly variation of land surface heat fluxes over the central Tibetan Plateau area. Theoretical Appl Climatology 80:259–273

Ma Y-M, Zhong L, Su Z-B, Ishikawa H, Menenti M, Koike T (2006) Determination of regional distributions and seasonal variations of land surface heat fluxes from Landsat-7 Ehanced Thematic Mapper data over the central Tibetan Plateau area. J GEOPHYS RES-ATM 111:D10305. doi:10.1029/2005JD006742

Ma Y-M, Kang S-C, Zhu L-P, Xu B-Q, Tian L-D, Yao T-D (2008) Tibetan observation and research platform—atmosphere–land interaction over a heterogeneous landscape. Bull Am Meteorol Soc 89:1487–1492

Ma Y-M, Menenti M, Feddes R (2010) Parameterization of heat fluxes at heterogeneous surfaces by integrating satellite measurements with surface layer and atmospheric boundary layer observations. Adv Atmos Sci 27(2):328–336

Montheith JL (1973) Principles of environmental physics. Edward Aarnold, London

Sato T, Kimura F (2007) How does the Tibetan Plateau affect the transition of Indian monsoon rainfall? Mon Weather Rev 135: 2006–2015

Valor E, Caselles V (1996) Mapping land surface emissivity from NDVI: application to European, African, and South American areas. Remote Sens Environ 57:167–184

Wang J, Ma Y-M, Menenti M, Bastiaanssen WGM (1995) The scaling-up of processes in the heterogeneous landscape of HEIFE with the aid of satellite remote sensing. J Meteorol Soc Jpn 73(6):1235–1244

Wu G-X, Zhang Y-S (1998) Tibetan Plateau forcing and timing of the monsoon onset over south Asia and South China Sea. Mon Weather Rev 126:913–927

Xu X-D, Lu C, Shi X-H, Gao S (2008) World water tower: an atmospheric perspective. Geophys Res Lett 35(20):L20815. doi:10.1029/2008gl035867

Yanai M, Li C-Y, Song Z (1992) Seasonal heating of the Tibetan Plateau and its effects on the evolution of the Asian summer monsoon. J Meteorol Soc Jpn 70:319–351

Yang K, Koike T, Ishikawa H, Ma Y-M (2004) Analysis of the surface energy budget at a site of GAME/Tibet using a single-source model. J Meteor Society Japan 82:131–153

Ye D-Z (1981) Some characteristics of the summer circulation over the Qinghai–Xizang (Tibet) Plateau and its neighborhood. Bull Am Meteorol Soc 62:14–19

Ye D-Z, Gao Y-X (1979) The meteorology of the Qinghai–Xizang (Tibet) Plateau. Science Press, Beijing, pp 1–278 (in Chinese)

Ye D-Z, Wu G-X (1998) The role of the heat source of the Tibetan Plateau in the general circulation. Meteorog Atmos Phys 67:181–198

Zhao P, Chen L (2001) Climate features of atmospheric heat source/sink over the Qinghai–Xizang Plateau in 35 years and its relation to rainfall in China. Science in China (D) 44:858–864

Zhong L, Ma Y-M, Suhyb Mhd SALAMA, Su Z-B (2010) Assessment of vegetation dynamics and their response to variations in precipitation and temperature in the Tibetan Plateau. Clim Chang. doi:10.1007/s10584-009-9787-8